SIMULATING GAS TURBINE BEARING FAILURE TOWARDS EFFECTIVE CONDITION MONITORING

By
*** Hyginus .U. Ugwu and ** Ezenwa .A. Ogbonnaya**

*** Department of Mechanical Engineering, Michael Okpara University of Agriculture, Umudike,**
Private Mail Box 7267, Umuahia, Abia State, Nigeria
Phone: 08064245409; E-mail: ubadyke2001@yahoo.com.au
Private Mail Box 5080, Nkpolu-Port Harcourt, Nigeria
Phone: 08023593123; E-mail: ezenwaogbonnaya@yahoo.com
**** Department of Marine Engineering, Rivers State University of Science and Technology,**

ABSTRACT
Recently, the requirements for the reliability of machines that perform different technological processes, their vibrational effects, and the failure of their bearings pose a great problem to gas turbine manufacturers and equipment owners. On most gas turbine plants, heavily-loaded slow rotating bearings are used which are in constant movement and vibration. A step-by-step method to the reduction of these vibrational forces led to this research. Thus, vibration readings were obtained from Afam power station to enuciate step towards resolving the problem. The data collected from the plant was hence used in the simulation of likely defects that could lead to down time resulting from vibration. A computer program code in Visual C#.Net was used to actualize the simulation. Results obtained show that early detection of imminent faults could help to prevent downtime. The results also show that the defect meted to the gas turbine depends on the amplitude of vibration measured at the bearing housing. Since the bearing at the turbine end carries more load than others, it should be constructed rigidly. Consequently, the results obtained further indicated that a speed of 3043 rpm is to be avoided due to the risk of resonance. Also, high vibrational amplitude was observed which can be attributed to the effect of imbalance. Generally, it is evident from the work that vibration analysis is very effective in condition monitoring of the health of a gas turbine and that its implementation is most efficient for detection and identification of incipient defects to its bearing.

Keywords: Bearing failure, Vibration analysis, Monitoring, Gas turbine, Resonance, Amplitude of vibration, Simulation.

NOMENCLATURE

A_i = Material property
T = A function of the contact surface dimensions
U = Number of stress cycle
D = Ball diameter, mm
D = Component (race way) diameter, mm
a^* = Function of major contact ellipse dimensions,
b^* = Function of minor contact ellipse dimensions,
T_i = Value of T when a*/b* = 1
S = Bearing characteristics number
r = Journal radius, mm
= Absolute viscosity, *Pa-S*
C = Radial clearance, mm
N = Significant speed, r/s
= Load per unit of projected bearing area, Mpa
$T_{(t)} = T_o sin\omega t$
$T_{(t)} = T_o cos\omega t$

1. INTRODUCTION

In the gas turbine (GT) components, the bearings are among the most important, and their exacting demands are made upon their load-carrying capacity and reliability. Bearings are highly reliable components and the vast majority of bearings will outlive the equipment on which they are installed. However, while

** Corresponding Author.

bearings account for a relatively small percentage of all equipment breakdowns, they do fail occasionally. When they fail, it is usually a critical event resulting in costly repair and downtime (Harris, 2005). Majorly, only a small number of bearing failures are caused by material failure. Fatigue serves more as a theoretical limit to bearing life than a real cause of bearing failure, indicating that they served a full life span (Loewenthal and Moyer, 1979).

Among the benefits resulting from this research is the ability to calculate the life of a bearing with considerable accuracy. This makes it possible to match the bearing life with the service life of the machine involved. Unfortunately, it sometimes happens that a bearing does not attain its calculated rated life. The many reasons for this included but not limited to heavy loading of bearing than anticipated, inadequate or unsuitable lubrication, careless handling, ineffective sealing or fits that are too tight, with resultant insufficient internal bearing clearance (Harris, 2005).

Each of these factors produces its own particular type of damage and leaves its own special imprint on the bearing. Consequently, by examining damaged bearing, it is possible in the majority of cases, to form an opinion on the cause of damage. Working towards the prevention of such damage in the future, thus becomes an effective source of condition monitoring (Ogbonnaya, 2004).

According to Rolforsagh, *et. al.* (2003), comprehensive prognostic capability can be achieved in bearings through the integration of health state awareness with model based damage assessments. The basis for this prediction is an intelligent fusion of diagnostic features and physics-based modeling. Since bearings have many failure modes as there are many influencing factors, a modular approach is taken in its design.

As stated above, there are many potential failure modes for bearings and a complete discussion of this failure is the scope of this project. Therefore, the normal bearing contact-fatigue failure mode herein called spalling is discussed. In addition, other failure modes that prematurely cause spalling conditions such as Brinnell marks resulting due to localized stress concentration in bearing are also discussed.

Some failure modes are not applicable to the prognostic architecture. Maintenance induced failures (misalignment, incorrect installation, etc) are impossible to predict. Contamination of the lubricant is one of the most common failure modes which becomes impossible to predict when contaminated. However, through sensor information, it is possible to detect the conditions that precede those failures such as detection of water in the lubricant, and by adjusting such prediction accordingly, the fatigue life would be predicted (Sahinkaya, et. al., 2001).

According to Sun, *et.al* (2004), the assessment of remaining life entails three functional steps namely, the design bearing health, current bearing health and future bearing health. The prediction process begins with the sensed data module. Signals indicative of the bearing health (vibration, oil debris, temperature, etc) are monitored to determine the current bearing conditions.

Moreso, bearing clearance and shaft misalignment can be checked in a variety of ways. A rough check is to observe the discharge of oil in the warm condition from the ends of the bearing. Feeler gauges can be used, but for some of the bearings, they can be difficult to manoeuvre into position in order to obtain readings. In consequence, clock gauges therefore can be very effective and accurate provision of the necessary relative degree of misalignment and movement would be achieved.

2. MATERIALS AND METHODS

The methodology and materials used to actualize this work are discussed in this section. This is done with a view to showing detailed steps used to give future researches a way forward.

2.1 Vibration

Vibration is the motion of a particle or a body which oscillates about its position of equilibrium. Most of the vibrations in a machine and structure are undesirable because of the increase in stresses and energy losses which accompany them. Vibration generally results when a system is displaced from a position of stable equilibrium. The system tends to return this position under the action of a restoring force (either elastic forces as in the case of mass attached to a spring, or gravitational forces as in the case of a pendulum).

The various types of vibration are as follows:

1. The free vibration
2. The forced vibration
3. The damped vibration and
4. The torsional vibration.

However, for the purpose of this research work, the free vibration and the damped vibration will be considered.

2.2 Free Vibration

Free vibration is a process where the motion is maintained by the restoring forces. This occurs when the particle is subjected to the force that is proportional to its displacement and in opposite direction. The oscillation system consists of a spring-mass system whose free body diagram (FBD) is shown in Fig.1.

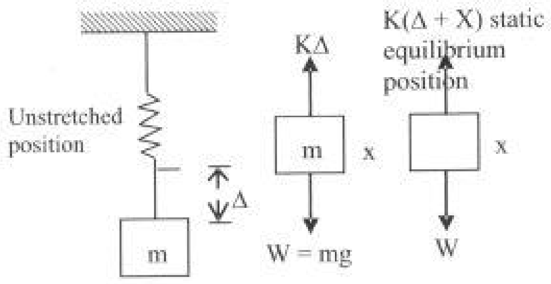

Fig. 1: A FBD of an oscillation system

The spring supporting the mass is assumed to be negligible in weight with a stiffness K, kg per unit deflection. The system possesses one degree of freedom since its motion is described by a single co-ordinate, x.

For a spring-mass system and its free body diagram (FBD), oscillation as a property of the system will occur at the natural frequency, w_n when the system is disturbed. If the deformation of the spring in the static equilibrium position is , and the spring force, K, is equal to the gravitational force, W acting on the mass, M as shown, then:

$$K \Delta = W \qquad (1)$$

Conversely, if X represents the displacement from the static equilibrium position and $K(+ X)$ is the upward and downward forces acting on the mass, while W becomes the weight, respectively, with x chosen to be positive in the downward direction, by applying Newton's second law of motion on the mass, m, equation (1) thus becomes

$$Mx = \sum F = W - K(\Delta + X) \qquad (2)$$

Hence, $K\Delta = -K\Delta$ (implied a restoring force that is equal and opposite to the applied force).

It is therefore evident that the choice of the static equilibrium position as references for x has eliminated the weight, W and the static force, K from the equation of motion, and the resultant force on mass, M is simply the spring force due to the displacement, X.

By mathematical definition, the period of oscillation of a simple harmonic motion (SHM), T is given by:

$$T = \frac{2\pi}{\omega} \qquad (3)$$

Thus, the frequency, f is

$$f = \frac{1}{T} = \frac{\omega}{2\pi} \qquad (4)$$

Comparing equations (3) and (4) by inversion gives:

$$\omega = \frac{2\pi}{T} = 2\pi f \qquad (5)$$

The resulting expression for the position of an object in SHM is stated as:

$$x(t) = A\sin(\omega t + \delta) \qquad (6)$$

Trigonometrically, Equation (6) can be rewritten as:

$$x(t) = [A\cos\delta]\sin(\omega t) + [A\sin\delta]\cos(\omega t) \qquad (7)$$

Also, since:

$$\sin(x + y) = \sin x \cos y + \cos x \sin y = \sin(\omega t + \delta)$$

By induction, Equation (7) becomes:

$$x(t) = a_1 \sin(\omega t) + a_2 \cos(\omega t) \qquad (8)$$

where $a_1 = A\cos\delta = x$ and $a_2 = A\sin\delta = y$ are constants obtained by comparing Equations (7) and (8).:

Specifying the position $x(t)$ as a function of time and taking successive derivatives, the velocity and the acceleration of the object in the SHM are obtained thus:

$$v(t) = \frac{dx}{dt} = \frac{d}{dt}[A\sin(\omega t + \delta)] = \omega A\cos(\omega t + \delta) \qquad (9)$$

and $a(t) = \frac{dv}{dt} = -\omega^2 A\sin(\omega t + \delta) = -\omega^2 x(t)$ (10)

Consequently, the spring force on a mass displaced by x from the equilibrium position of the spring is a restoring force linearly dependent on x, the form known as Hooke's law and given by Fishbane et.al. (2005) as:

$$F = -Kx \qquad (11)$$

This form is valid provided the spring is not overly stretched or compressed, in which case, it loses its "springiness" and distorts. Here, K is the spring constant. The minus sign indicates that the force is a restoring force and a displacement in the $+x$ -direction gives rise to a force that acts in the $-x$ -direction and vice versa.

Based on Newton's second law of motion, the connection between the force and the acceleration when the mass is released at $t = 0$ om an extended position over a complete period of the motion is thus:

$$F = -Kx = ma \qquad (12)$$

Hence, the acceleration of a mass on the end of a spring is proportional to its displacement with a minus sign and stated as:

$$a = \frac{-K}{m}x \qquad (13)$$

Comparing Equations (10) and (13) yields an important result that the angular frequency is determined by the mass and the spring constant. Thus

$$\omega^2 = \frac{k}{m} \qquad (14)$$

$$\therefore \quad \omega = \sqrt{\frac{k}{m}} \qquad (15)$$

Conversely, comparing Equations (3) and (4) give the period and the frequency of the oscillations expressed respectively as:

$$T = 2\pi\sqrt{\frac{m}{k}} \qquad (16)$$

and $$f = \frac{1}{2\pi}\sqrt{\frac{k}{m}} \qquad (17)$$

These, suggest remarkably that the period of the motion and the frequency of oscillation are independent of the amplitude of the vibration.

2.3 Damped Vibration

Fig. 2 is the FBD of a damped vibration. In this type of vibration, a linear system of one degree of freedom is excited. Its response will depend on one of excitation and damping which is represented in the FBD by the equation of motion given as:

$$M\ddot{x} + C\dot{x} + Kx = f(t) \qquad (18)$$

where: f(t) is the excitation and $C\dot{x}$ is the damping force, while C is a constant. If $f(t)=0$, it is homogenous.

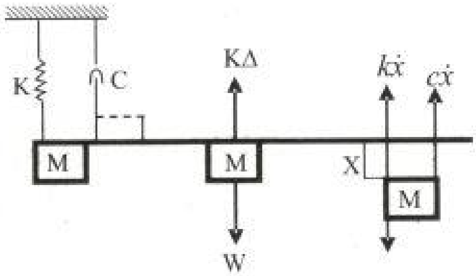

Fig.2: FBD of a damped vibration

The exciting force is supplied by the rotation of an imbalance eccentric mass *"m"* with eccentricity *"e"*. The machine can be modeled as a spring-mass rotating machinery as shown in Fig. 3.

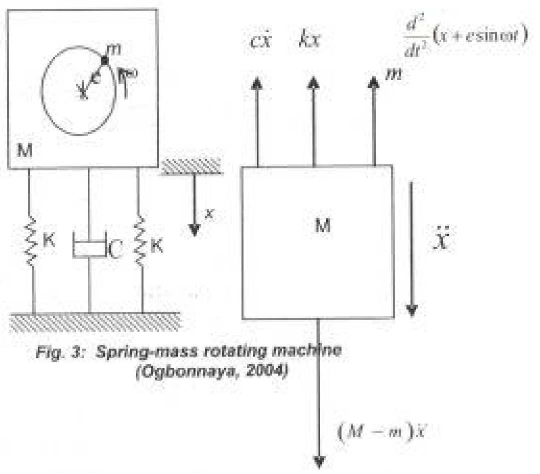

Fig. 3: Spring-mass rotating machine (Ogbonnaya, 2004)

From the above diagram, the amplitude of the vibration caused by the imbalance can be systematically generated from:

$$M\ddot{x} + C\dot{x} + Kx = F_0 \sin(\omega t) \qquad (19)$$

where:
M = total mass of the system including m
C = viscous damping coefficient
K = spring stiffness constant
F_0 = impressed/exciting force and
x = displacement of spring supported mass.

By mathematical computation, the amplitude X of the vibration can be expressed as follows:

$$X = \frac{F_0}{\sqrt{(k-M\omega^2)^2 + (c\omega)^2}} \qquad (20)$$

But the exciting force, F_0 is generated by the imbalance mass, m. Therefore, the force can be expressed as:

$$F_0 = me\omega^2 \qquad (21)$$

where:
m = imbalance mass,
e = eccentricity,
$\omega = \frac{2\pi N}{60}$
= frequency of the excitation force, rad/sec; and N = Speed in rpm.

Hence, Equation (20) now becomes:

$$X = \frac{me\omega^2}{\sqrt{(k-M\omega^2)^2 + (c\omega)^2}} \qquad (22)$$

Thus, based on Equation (22), the flowchart of the computer program used to simulate the vibration displacement amplitude of the turbine and speed as depicted in Fig. 4 was generated. The iteration was carried out about 13times before the cycle could complete.

3. RESULTS AND DISCUSSION

3.1 Simulation of Afam GT Unit 17

Gas turbine [GT unit 17] was healthy until there was a bearing failure. Therefore, readings of vibration velocity amplitude [mm/sec] on the bearings 1-3 were taken from GT 17 of Afam power station as presented in table 1. The design and manufacture characteristics of the plant is shown in Appendix I, while the program code in Visual C#.NET and the results of the vibration displacement amplitude (mm) of the engine are shown in Appendices II and III, respectively.

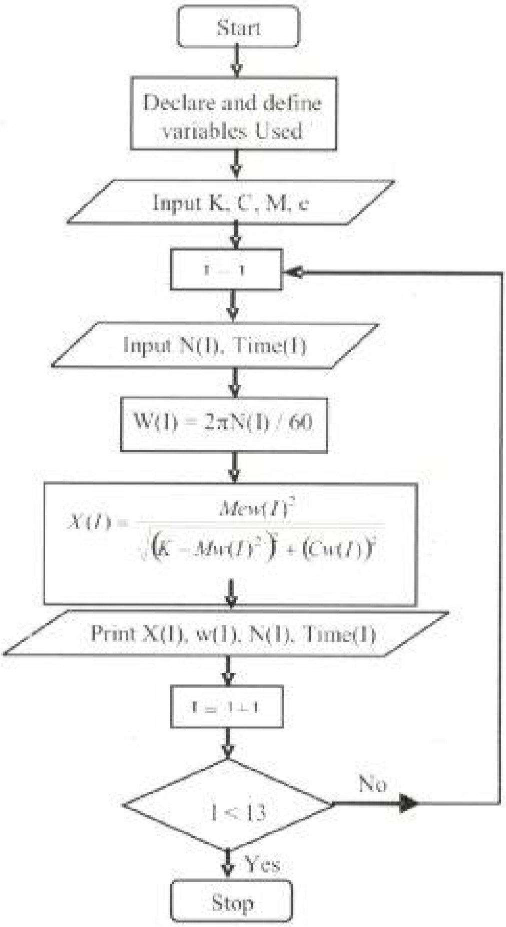

Fig. 4: Program code in Visual C#. NET programming language

N	W	Active Load	XP	Bearing 1	Bearing 2	Bearing 3
2977	50.1	51	0.3999993815	4.7	1.0	6.4
2980	49.8	50	0.3999993732	5.2	1.0	6.5
2983	49.8	51	0.3999993728	5.4	0.9	6.6
2986	49.7	51	0.3999993711	5.4	0.9	6.7
2989	49.9	51	0.3999993740	5.1	1.0	6.6
2992	50.1	51	0.3999993782	4.8	0.9	6.5
2995	50.1	52	0.3999993627	4.8	0.9	6.4
2998	50.1	51	0.3999993774	4.9	1.0	6.6
3001	50.6	51	0.3999993880	4.8	1.0	6.6
3004	50.1	50	0.3999993765	4.8	1.1	6.6
3007	50.1	49	0.3999993757	4.5	1.2	6.7
3010	50.1	47	0.3999993778	4.6	1.2	6.7
3013	49.8	48	0.3999993728	4.9	1.2	6.7
3016	49.9	48	0.3999993711	4.9	1.2	6.8
3019	50.2	50	0.3999993778	5.0	1.0	6.6
3022	50.1	50	0.3999993778	5.0	1.0	6.6
3025	50.4	49	0.3999993827	4.7	1.0	6.5
3028	50.2	48	0.3999993786	4.9	1.0	6.6
3031	49.9	48	0.3999993698	5.6	1.0	6.7
3034	49.6	48	0.3999993660	6.0	1.0	6.6
3037	49.9	48	0.3999993715	5.5	1.0	6.7
3040	50.8	48	0.3999993968	3.9	1.0	6.4
3043	49.5	49	0.3999993643	6.1	0.9	6.8
3046	49.8	48	0.3999993729	5.4	1.0	6.7

3.2 GT Unit 17

The results of the data collected as shown in table 1 are used in plotting the graph of the vibration amplitude of the three bearings of GT 17 against the variation of their shaft speed as presented in Fig.5. From the graph, it is observed that the amplitude at various bearings is almost constant as the speed of the turbine increases. This is so as there is no eccentricity to cause any imbalance. However, the markedly high vibration amplitude on bearing 1 can be atttributed to the effect of imbalance in the turbine rotor and coupling along the shaft. Therefore, this bearing is prone to fail if it is not checked. Hence, why bearing 1 has the highest vibrational amplitude.

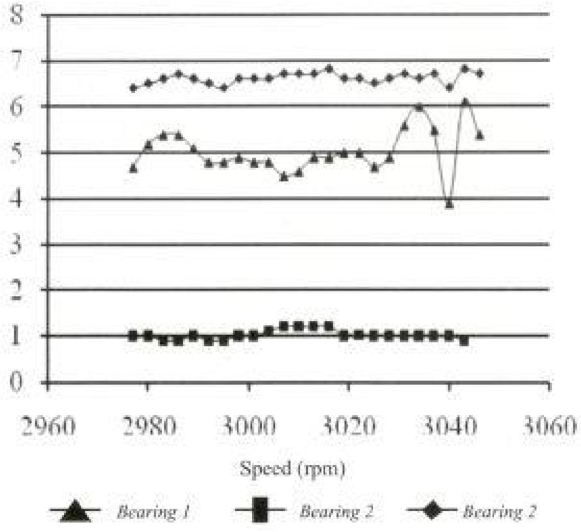

Fig 5: Vibration amplitude for bearing 1,2,3 aganist turbine speed.

3.3 Simulation of Bearing 1

Fig. 6 is a graph of vibrational amplitude of bearing 1 against its rotational speed (rpm). From the graph, it is observed that there is an upward and a corresponding downward movement, resulting to slight change of vibration peaks at various vibration amplitude and rotational speed. Maximum vibration occurs at 3043rpm which should be avoided when running the engine so as to avoid breakdown.

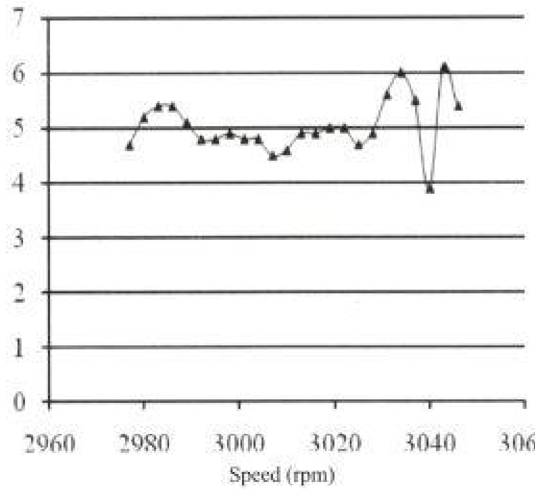

Fig. 6: Vibration amplitude of bearing 1 aganist rotational speed.

3.4 Simulation of Bearing 2

A graph of vibrational amplitude of bearing 2 aganist the rotational speed is shown in Fig 7. It is observed from the graph that the vibration peaks are constant between the speed of 3015 to 3018rpm. The engine is not advisable to run at such speed so as to avoid eccentricity and the risk of resonance.

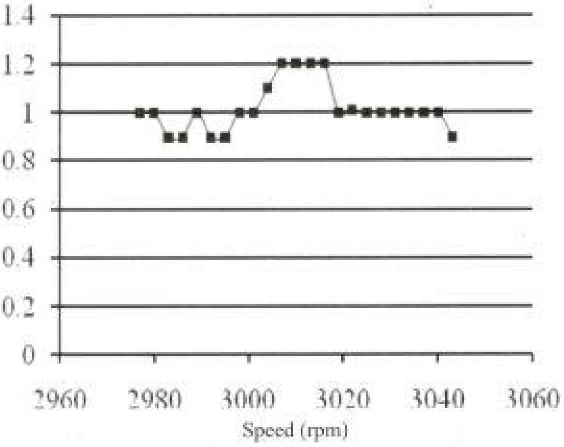

Fig. 7: Vibration amplitude of bearing 2 aganist rotational speed

3.5 Simulation of Bearing 3

Looking at the result of the graph of the vibration amplitude of bearing 3 against the turbine rotational speed from Fig 8, it is observed that rotational speed is increasing rapidly from every vibration point. The peaks at various points shown represent the vibration points. An increase in rotational speed results to a corresponding change in vibrational amplitude of the gas turbine and vibration is maximum at about 3043rpm. It is not advisable for the engine to run at such speed so as to avoid imbalance and eccentricity of the engine.

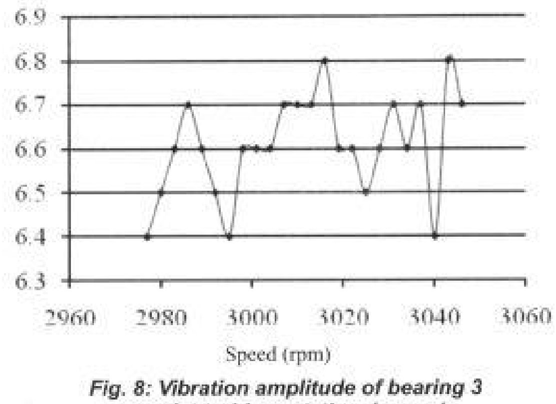

Fig. 8: Vibration amplitude of bearing 3 aganist turbine rotational speed.

3.6 Load Analysis of The Engine

Fig 9 shows the graph of Active load against the turbine speed. The load fluctuates with increasing speed. This shows that the level of vibration in an engine while in operation is determined by the loading. Hence the sudden removal of the load results in reduction or increase in vibration amplitude and also causes increase in torsional stress on the shafting system.

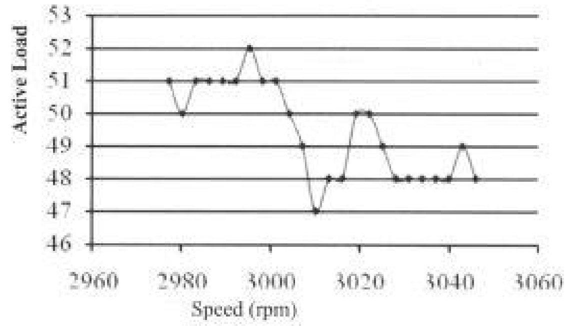

Fig 9: Active load aganist turbine speed

4 CONCLUSION AND RECOMMENDATIONS

4.1 Conclusion

A work on analysis of bearing behaviour of a GT plant has been carried out. Results thus have shown that monitoring the health of the bearings can help in the prevention of downtime of a GT plant.

The bearing at the turbine end of the GT plant carries much load and thus high vibration amplitude occurs there. So, a step-by-step analysis of plant parameters obtained was used to write a program on visual C#.Net to determine the vibration displacement amplitude of the plant.

It was also found out that the amount of defect meted to the GT depended on amplitude of vibration and friction as measured at the bearing housings. The work also revealed that vibration diagnostics is most efficient for detection and identification of incipient defects in bearings. Therefore, vibration analysis is very effective in condition monitoring of GTs.

4.2 Recommendations

From the results obtained in this work, the following reommendations are made:

The performance of GT bearings should be monitored during the engine operation.
A software should be produced to monitor the vibration amplitude of the bearings.
The bearing at the turbine side should be rigidly constructed.

ACKNOWLEDGEMENTS
Our gratitude goes to Miss Epelle, Ibelema Queen of the Department of Marine Engineering in Rivers State University of Science and Technology, Nkpolu, Port Harcourt for her ingenuity exhibitted in the data collection and experimentations that led to the success of this paper. Also, we thank Mr. Ogbonnaya of Afam Power Station for his support and the provision of data used in this analysis.

REFERENCES

Fishbane, Paul M; Gasiorowicz, Stephen G; and Thornton, Stephen T. (2005). *Physics for Scientists and Engineers with Modern Physics, 3rd Edition: International Edition,* Pearson Prentice Hall Inc; Publishers, New Jersey, USA; pp. 366-389.

Harris, T. (2005). *Rolling Bearing Analysis,* 4th Edition, John Willy & Sons, New York; pp 34-40.

Loewenthal, S. and Moyer, D. (1979). *Filtration Effects on Bearing Life and Condition in a Contaminated Lubricant,* Journal of Lubrication Technology, Transactions of the ASME, Vol.101, pp.171-179.

Ogbonnaya, E. A. (2004). *Modeling Vibration Based Fault on Rotor Shaft of Gas Turbine*, PhD Thesis, Department of Marine, RSUST, PortHarcourt, pp. 35-40.

Rolforsagh, F. Scheldon; Jeremy, Wenke; and Christopher, J. (2003). *Prognostics/Diagnostics for Gas Turbine Engine Bearings,* Proceedings of STLE Annual Meeting, New York, NY.

Sahinkaya, M.N; Cole, O.T; and Burrows C.R. (2001). *Fault Detection and Tolerance in Synchronous Vibration Control of Rotor-magnetic Bearing System,* Proceedings of the Institution of Mechanical Engineers, Part C: Journal of Mechanical Engineering Science, Vol.215, No.12, pp. 1401-1416.

Sun, Q; Chen, P; Zhang, D; and Xi, F. (2004). *Pattern Recognition for Automatic Machinery Fault Diagnosis,* Journal of Vibration and Acoustics, Vol.126, No.2, pp.307-316.

APPENDIX I
ENGINE CHARACTERISTICS

Rotor Shaft:
1. Compressor Shaft = 1308mm
2. Turbine Shaft = 1990mm
3. Generator Shaft = 1080.4mm

Mass of Rotors:
1. Compressor Rotor Weight = 61,190 KN(6,240kg)
2. Turbine Rotor Weight = 6234kg

Spring Constant of Shaft, K = 20KN.m/Rad
Area of Shaft 36.08m
Bearing Damping Coefficient, C=3502Ns/m (over-damped), 1.0Ns/m (Under Damped)
Density = 76850kg/m^3
Modulus of Rigidity, G = 80GN/m^2
Modulus of Elasticity, E = 207GN/m^2
Mass Moment of Inertia, I = 332.71m^4
Design engine speed = 3000rpm

APPENDIX II
Program Code in Visual C#.NET Programming Language

```
using System;
using System.Collections.Generic;
using System.Linq;
using system.Text;
namespace ConsoleApplication1
{
        Class Program
        {
                Static void Main(strings[] args)
                {
                        double K, C, M, e, w, pi, bb;
                        double[] X 0 new
double[24];
                        double [] N =
{3018,2998,2997,2993,3000,3010,3021,3008,3034,
3006,3004,3009,2997,2993,3009,

3009,3021,3011,2990,2981,

                        2994,3056,2977,2997
int i;
                        pi = 22/7.0;
                        K = 20.0;
                        C = 3502.0;
                        M = 6234.0;
                        e = 0.4;
                        Console.WriteLine("   N
w   X");
Console.WriteLine("==========================");
        for (i = 0; i < 24; i++)
        {
                W = 2 * pi * N[i] / 60.0;
                bb = ((K - (M * w * w))        * (K -
(M * w * w))) + (C * w * C * w);
        X[i] = (M * c * w * w) / Math.Sqrt(bb);
        Console.WriteLine("{0,10:f2},{1,10:f2},

{2,14:f10}",N[i],w,X[i]);
                        }
        Console.ReadLine( );
                }
        }
}
```

Select file:///C:/Users/FibzGlobal/Documents/Visual Studio 2008/Projects/ConsoleApplication1/Co...

N	w	X
3018.00,	316.17,	0.3999993815
2998.00,	314.08,	0.3999993732
2997.00,	313.97,	0.3999993728
2993.00,	313.55,	0.3999993711
3000.00,	314.29,	0.3999993740
3010.00,	315.33,	0.3999993782
3021.00,	316.49,	0.3999993827
3008.00,	315.12,	0.3999993774
3034.00,	317.85,	0.3999993880
3006.00,	314.91,	0.3999993765
3004.00,	314.70,	0.3999993757
3009.00,	315.23,	0.3999993778
2997.00,	313.97,	0.3999993728
2993.00,	313.55,	0.3999993711
3009.00,	315.23,	0.3999993778
3009.00,	315.23,	0.3999993778
3021.00,	316.49,	0.3999993827
3011.00,	315.44,	0.3999993786
2990.00,	313.24,	0.3999993698
2981.00,	312.30,	0.3999993660
2994.00,	313.66,	0.3999993715
3056.00,	320.15,	0.3999993968
2977.00,	311.88,	0.3999993643
2997.00,	313.97,	0.3999993728

APPENDIX III
VIBRATIONAL DISPLACEMENT AMPLITUDE OF THE TEST ENGINE